TEXHIKA TA METOДИ ЕКСПЕРИМЕНТУ ENGINEERING AND METHODS OF EXPERIMENT

УДК 539.1+616-006

https://doi.org/10.15407/jnpae2025.03.272

K. Vilchynska^{1,2}, O. Bezshyyko¹, L. Golinka-Bezshyyko^{1,*}, R. Zelinskyi³

¹ Taras Shevchenko National University of Kyiv, Kyiv, Ukraine
² Radiotherapy Department, Universal Clinic "Oberig", Kyiv, Ukraine
³ Radiotherapy Department, Medical Center of Yuriy Spizhenko LLC, Kyiv, Ukraine

*Corresponding author: lyalkagb@gmail.com

COMPARISON OF DOSE DISTRIBUTIONS MEASURED WITH DIFFERENT DETECTORS IN LARGE AND SMALL RADIATION FIELDS

The study investigates the dose distributions in large $(10 \text{ cm} \times 10 \text{ cm})$ and small $(1 \text{ cm} \times 1 \text{ cm})$ radiation fields, comparing calculated and measured data using two detectors. Special attention is given to the impact of source occlusion in small fields and the phenomenon of penumbra overlap, as predicted by theoretical models. Small radiation fields, crucial in clinical radiation therapy, present unique challenges in dosimetry due to these effects. The results highlight the discrepancies between large and small fields, emphasizing the importance of precise measurement and the limitations of current dosimetric equipment in small-field applications.

Keywords: radiation therapy, quality assurance, detectors, radiochromic film, linear accelerator, treatment planning system, dose distribution.

1. Introduction

Small field dosimetry presents unique challenges distinct from those encountered in broad beam dosimetry. The deviations arise due to the loss of lateral charged-particle equilibrium (LCPE), partial source occlusion, and the limitations of existing detector technologies. These issues critically affect dosimetric accuracy, impacting clinical outcomes and treatment planning system (TPS) data reliability. This article examines these challenges, with particular emphasis on source occlusion, penumbra overlap, and detector-related limitations.

A radiation field is classified as small when its dimensions are less than the lateral range of charged particles, leading to a loss of LCPE.

The IAEA TRS-483 [1] defines specific criteria to identify small fields. There should be a loss of LCPE on the beam axis, partial occlusion of the primary photon source by the collimating devices on the beam axis, and the size of the detector should be similar to or larger than the beam dimensions. The first two characteristics are beam related, while the third one is detector-related for a given field size. All three of these conditions result in overlap between the field penumbrae and the detector volume.

Achieving charged-particle equilibrium becomes critical; for this, the full-width at half-maximum (FWHM) of the field must exceed twice the lateral charged-particle range plus the detector's boundary distance to the field edge (Fig. 1).

Partial source occlusion occurs when the source size and beam geometry lead to overlapping penumbrae in small fields. This has several dosimetric consequences. The actual field size, as determined by FWHM, can deviate from the nominal collimator-defined field size, complicating TPS data. Machine output decreases as the beam spot becomes partially occluded (Fig. 2). Smaller fields reduce head and phantom scatter, filtering out low-energy photons and increasing the mean energy. Studies, such as [2], underline the significant impact of these effects on clinical dosimetry.

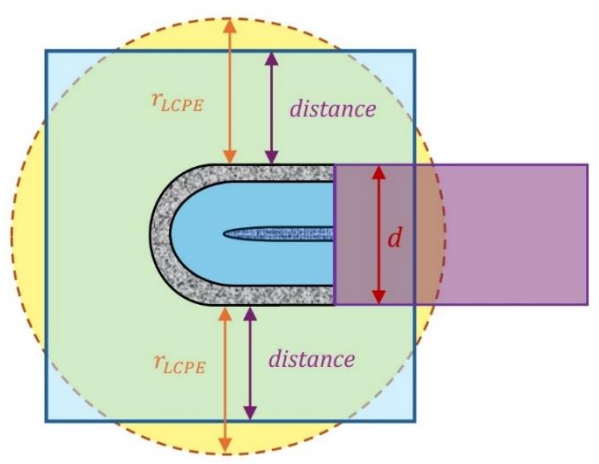


Fig. 1. To achieve charged-particle equilibrium, the condition FWHM $\geq 2 \cdot r_{LCPE} + d$ must be met, where d is the diameter of the ionization chamber. (See color Figure on the journal website.)

Detectors designed for broad beams often underperform in small fields due to the following limitations. Ionization chambers, the backbone of radiation therapy dosimetry, average signals over their volume, which is problematic in high-dose gradient regions [3]. These chambers require significant corrections to account

The Author(s), 2025

Published by INR of NAS of Ukraine as an open access article under the CC BY-NC 4.0 license

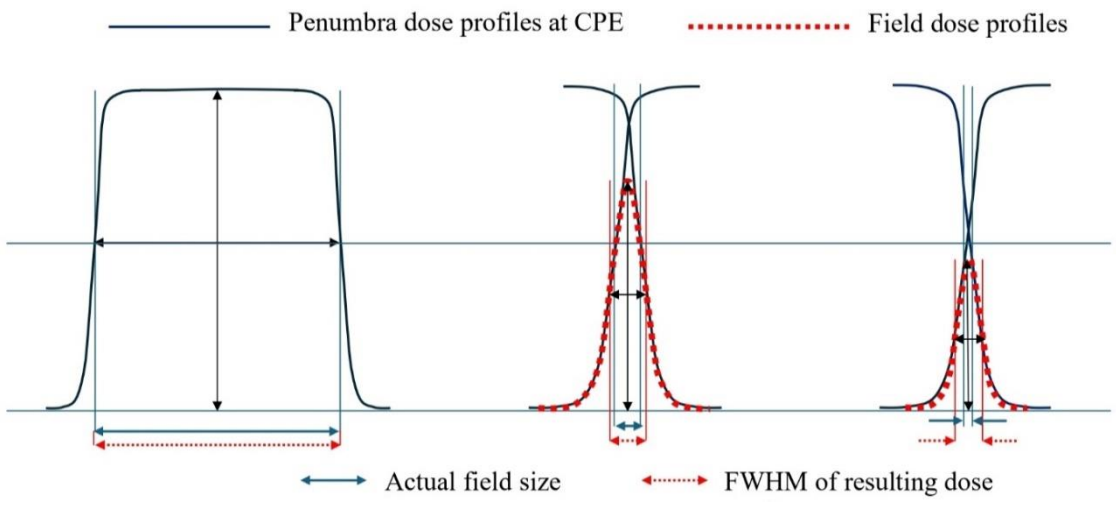


Fig. 2. Illustration of penumbra overlapping in small field dosimetry. The blue arrows represent the collimator-defined field size, while the red dashed arrows show the resulting actual field size due to penumbra effects. (See color Figure on the journal website.)

for fluence perturbations and non-uniform dose distributions around the sensitive volume. To reduce disturbances and averaging effects, chambers need to be small enough to avoid significant interference, while still maintaining sufficient sensitivity for accurate measurements. Solid-state detectors, such as silicon diodes and diamond detectors, offer advantages such as smaller sensitive volumes and higher spatial resolution. However, their performance is affected by material properties, requiring substantial correction factors to achieve dosimetric accuracy.

In clinical practice, array detectors such as MatriXX Evolution are commonly used for treatment plan verification and, when the sensitive volume of an individual detector element is smaller than the radiation field size, they can also be applied to small-field measurements. Nevertheless, their spatial resolution is essentially limited by the size and spacing of the detectors. For studies requiring significantly higher spatial resolution – two to three orders of magnitude greater – micro-pixel detectors offer a more suitable alternative. Examples include the PantherPix hybrid pixel γ -ray detector [4], the TimePix metal microdetector [5], and the PILATUS single-photon counting pixel detector [6].

The Bragg-Gray cavity theory and related formulations assume charged-particle equilibrium and small, independent perturbation correction factors. In small fields, these assumptions often break down. The fluence in the medium differs from that in the detector due to variations in mass stopping powers and design-related factors, such as high-Z materials surrounding the sensitive volume. Correction factors in small fields can reach up to 10 %, significantly affecting dose accuracy. Monte Carlo (MC) simulations have proven invaluable in modeling these effects, enabling better understanding and quantification of perturbation factors.

In broad beams, field output factors are typically calculated as the ratio of detector readings in clinical and reference fields. This approach fails in small fields due to the non-constancy of stopping power and perturbation ratios [7]. The concept has been redefined to incorporate MC-calculated or experimental correction factors to ensure accurate dose ratios between small and reference fields. The IAEA TRS-483 report emphasizes these corrections, providing guidelines for reliable dosimetry in small fields, including recommendations on suitable detectors and their calibration.

Small field dosimetry is fundamentally complex, with significant challenges coming from source occlusion, penumbra overlap, and detector limitations. While solid-state detectors address some of these issues, the accurate quantification of perturbation factors remains crucial. The adoption of MC-simulations to protocols like [1] can enhance dosimetric precision, ultimately improving clinical outcomes in radiotherapy. Further research and development of novel detectors specifically designed for small fields are essential to address existing gaps and advance the field of radiation therapy dosimetry.

2. Experimental measurements

2.1. Methodology

A plan was developed using the Eclipse TPS (Varian, version 16.1). A photon beam was delivered by a Varian TrueBeam STx linear accelerator equipped with a multileaf collimator for beam shaping. The gantry and collimator angles were set to 0°. Two field sizes were investigated: a standard

 $10 \text{ cm} \times 10 \text{ cm}$ field and a small $1 \text{ cm} \times 1 \text{ cm}$ field. For both cases, the dose prescribed was 9 Gy, and the Acuros XB algorithm calculated the particle fluence required to deliver this dose to a depth of 5 cm within a heterogeneous medium. The radiation fields were created using 6 MeV photon beams with a flattening filter (WFF).

The Acuros XB (eXtended Boltzmann) algorithm is a deterministic dose calculation method that solves the Linear Boltzmann Transport Equation to accurately model radiation transport [8]. Unlike traditional algorithms, it explicitly considers tissue heterogeneities and material composition, offering improved precision in small-field and heterogeneous geometries. It calculates dose by directly modeling the physical interactions of photons and electrons with matter, rather than relying on empirical dose kernels or simplified assumptions.

2.2. Equipment

2.2.1. Gafchromic EBT3

A RW3 Slab Phantom was used to reproduce tissue-equivalent properties. Gafchromic EBT3 film, characterised by high spatial resolution (up to 25 μ m) and energy independence for photon energies above 100 keV, was employed to measure dose distribution [9]. The phantom and film were arranged as follows: three RW3 slabs, each 1 cm thick, were placed below the EBT3 film to account for backscatter effects from the treatment couch (Fig. 3). Five RW3 slabs, each 1 cm thick, were placed above the film to simulate a measurement depth of 5 cm. The entire setup was scanned using a Siemens Healthineers CT scanner. The scan data provided Hounsfield Units (HU) for the materials, which were subsequently converted into material densities for use in the simulation.

A multileaf collimator system on the Varian TrueBeam STx was used to shape the radiation fields (Fig. 4).

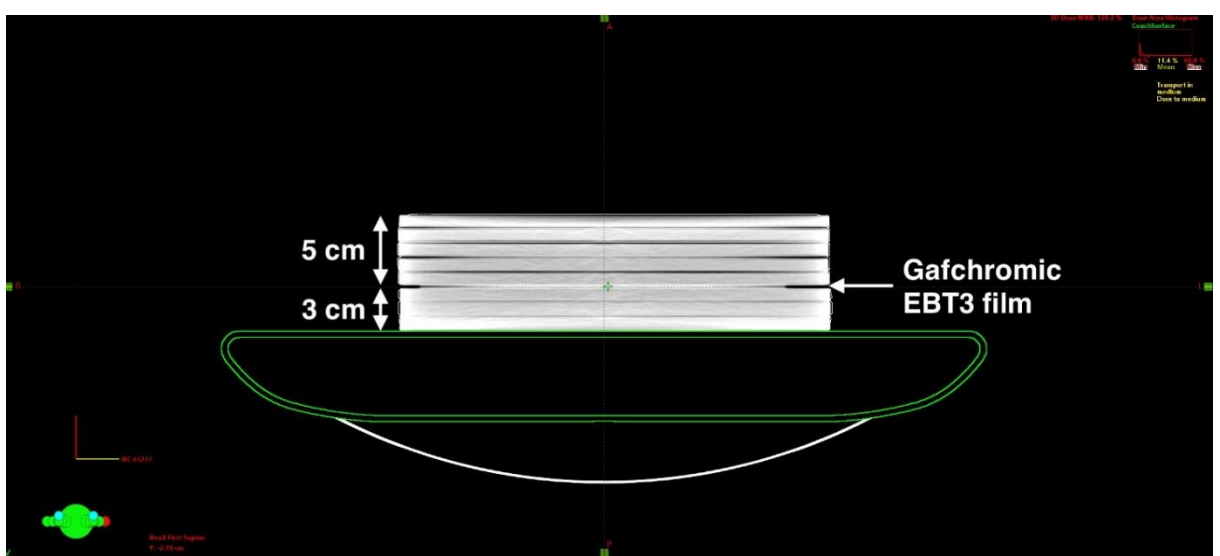


Fig. 3. Setup for dose distribution measurement using Gafchromic EBT3 film in an RW3 Slab phantom: illustration of backscatter and measurement depth simulation. (See color Figure on the journal website.)

Unlike jaw collimation, a multileaf collimator enables greater flexibility in defining irregular or small fields. The TrueBeam STx is equipped with a high-precision multileaf collimator, capable of achieving a leaf positioning accuracy of less than 1 mm [10]. The overlapping penumbrae of adjacent leaves and the finite leaf width significantly influence dose distributions, particularly in small fields such as $1 \text{ cm} \times 1 \text{ cm}$.

Comparisons were made between theoretical aspects described in [1] and the measured dose profiles. Particular attention was given to the following phenomena: source occlusion, observed as attenuation in the central axis dose due to partial multileaf collimator coverage of the source; penumbra overlap,

studied to understand its contribution to dose uniformity and gradient steepness in small fields; and loss of LCPE, quantified to evaluate its impact on dose accuracy in the 1 cm \times 1 cm field.

The CT scan was performed with a slice thickness of 3 mm, ensuring high-resolution imaging for accurate HU-to-density conversion. The Siemens Healthineers scanner's advanced reconstruction algorithms ensured precise characterisation of material properties, which is critical for dose calculations.

Gafchromic EBT3 film has a thickness of 0.28 mm, a dynamic dose range up to 40 Gy, and water equivalence for photon energies. The RW3 Slab Phantom is a tissue-equivalent material with a density of 1.045 g/cm³.

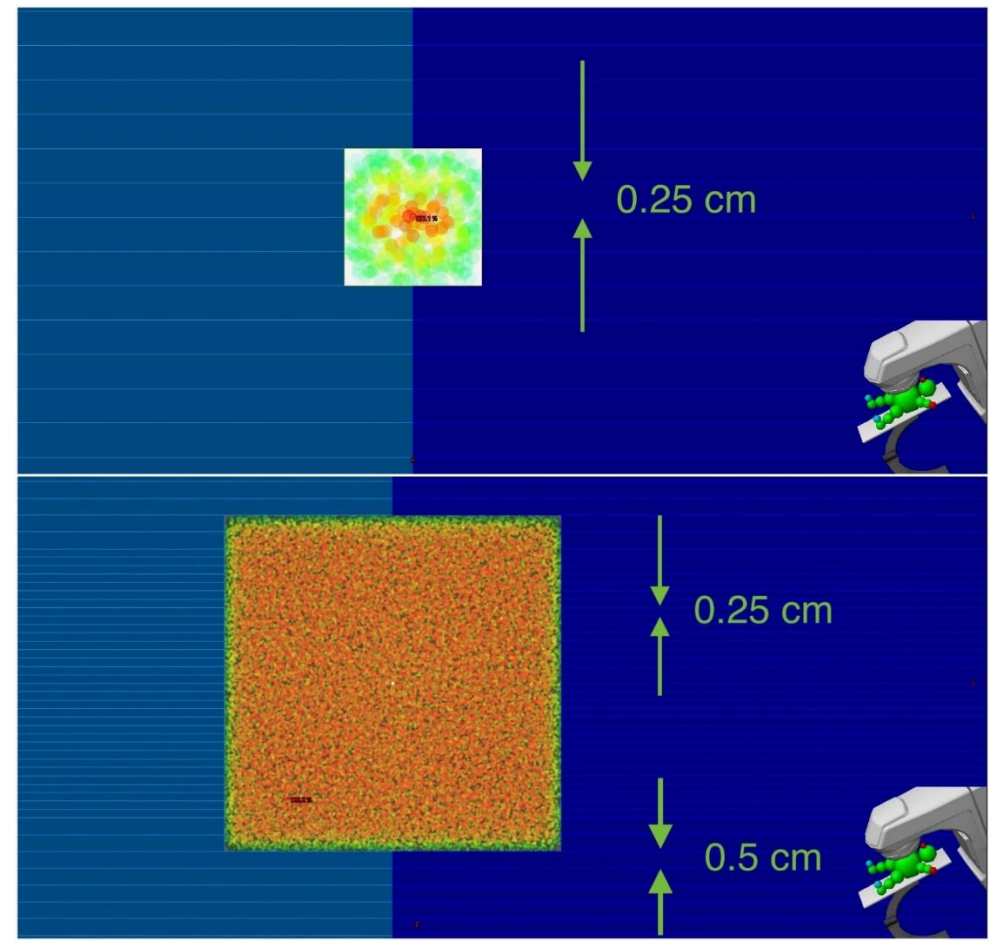


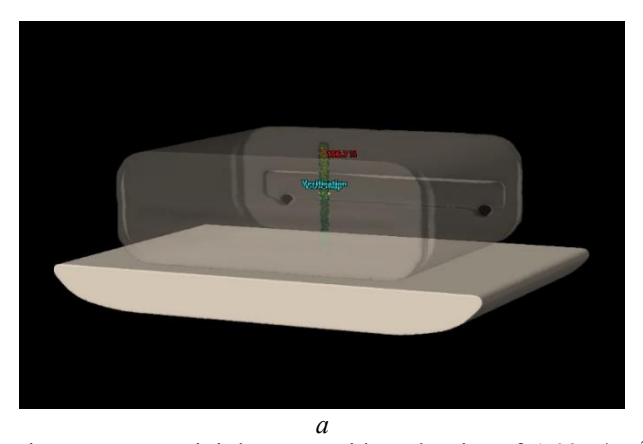
Fig. 4. Radiation fields of 1 cm \times 1 cm and 10 cm \times 10 cm shaped by the TrueBeam's multileaf collimator. The central leaves have a thickness of 0.25 cm, while the peripheral leaves are 0.5 cm thick, ensuring precise field shaping for small and large radiation field sizes. (See color Figure on the journal website.)

2.2.2. MatriXX Evolution

MatriXX Evolution detector, a product of IBA Dosimetry, was utilized as the second detector to verify dose profiles from $1~\text{cm} \times 1~\text{cm}$ and $10~\text{cm} \times 10~\text{cm}$ radiation fields during this measurement. This detector is designed with 1020 ionization chambers arranged in a high-resolution two-dimensional grid, each chamber spaced approximately 7.6 mm apart [11]. To prepare

the detector for use, it was first scanned with a Siemens Healthineers CT scanner to obtain Hounsfield unit data. These Hounsfield unit values were then converted into material densities for use in simulations.

During the experiment, MatriXX Evolution was positioned within a miniPhantom with a density of 1.03 g/cm³ to simulate realistic treatment conditions (Fig. 5).



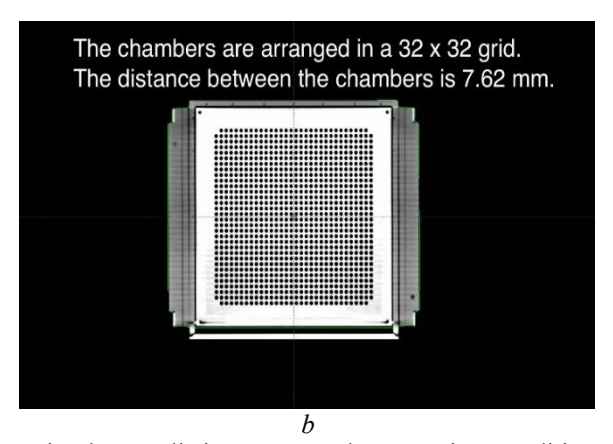


Fig. 5. a – A miniPhantom with a density of 1.03 g/cm³ to simulate realistic scatter and attenuation conditions. b – MatriXX Evolution detector consists of 1020 ionization chambers uniformly distributed across an area of 24.4 × 24.4 cm². The device also incorporates a buildup material on top, which is 6 mm of ABS Tecaran (a terpolymer and an amorphous resin). (See color Figure on the journal website.)

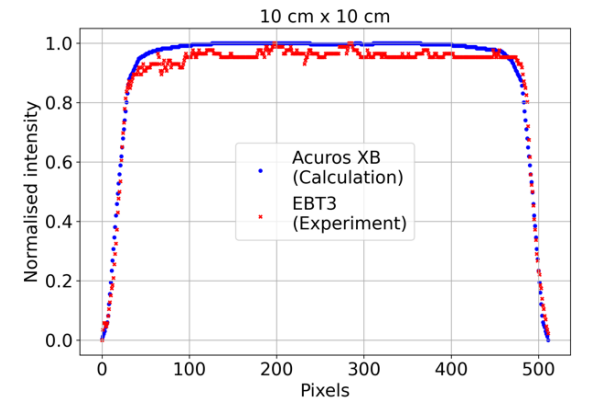
MiniPhantom ensured appropriate scatter conditions, accounting for both backscatter and attenuation effects. The detector's output was analyzed to assess the accuracy of dose delivery, with measurements compared against the calculated dose distributions.

3. Results

3.1. Analysis of dose profiles using EBT3 film

Using the TPS, the dose plane was exported for comparison. To match the film's high resolution, the calculated dose distribution was exported from the TPS with the finest resolution available. Python code was employed to align and compare the calculated and experimentally measured 2D dose distributions.

To ensure a meaningful comparison, the dose profiles obtained from the Gafchromic EBT3 film and



normalization was performed using the equation:

$$I_{normalised} = \frac{I - I_{min}}{I_{max} - I_{min}},\tag{1}$$

where *I* represents the intensity or dose value at a given point, I_{min} is the minimum intensity value, and I_{max} is the maximum intensity value within the profile. This method scales the profiles between 0 and 1, ensuring a consistent baseline for comparison and highlighting spatial differences in the dose distributions.

those calculated by the TPS were normalized. The

Horizontal dose profiles were extracted from the films for the 1 cm \times 1 cm and 10 cm \times 10 cm fields. Comparisons were made between the calculated and measured profiles for each field size, providing insights into the accuracy and reliability of the TPS and Acuros XB calculations (Fig. 6).

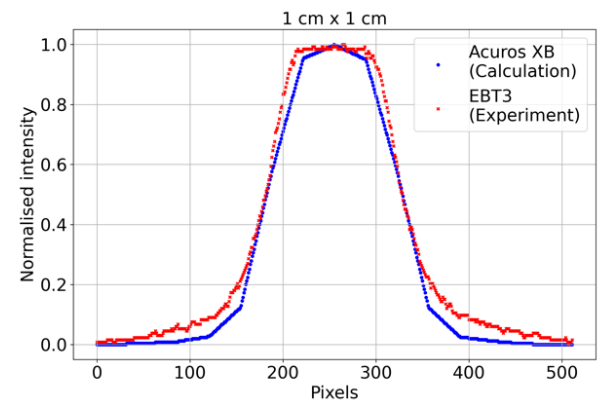


Fig. 6. Comparison of dose profiles: the calculated curve from the TPS and the measured curve from the Gafchromic EBT3 film. (See color Figure on the journal website.)

The comparison between the dose profiles calculated by the TPS and those measured with the Gafchromic EBT3 film revealed a mean relative error (MRE) of 49.97 %. This deviation was calculated using Python, where the relative differences between the two profiles were determined at each corresponding data point. The MRE was computed using the equation:

$$MRE = \frac{1}{N} \sum_{i=1}^{N} \left| \frac{I_{TPS,i} - I_{Film,i}}{I_{TPS,i}} \right| \cdot 100\%,$$
 (2)

where $I_{TPS,i}$ and $I_{Film,i}$ are the dose values at the *i*-th point for the TPS and film profiles, respectively, and N is the total number of points.

The equation for the standard deviation between two curves can be represented as follows:

$$\sigma = \sqrt{\frac{1}{N} \sum_{i=1}^{N} (I_{TPS,i} - I_{Film,i})^{2}} .$$
 (3)

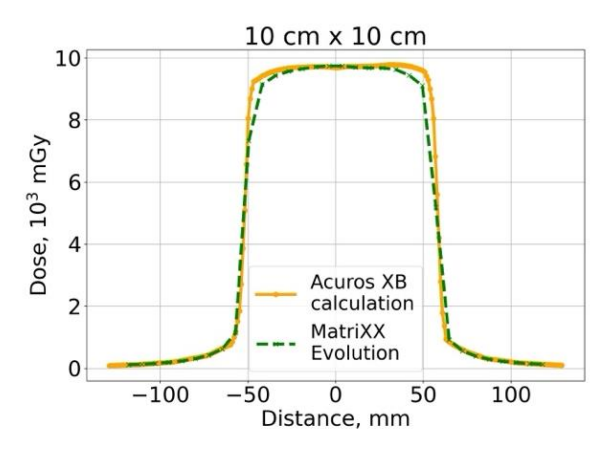
Comparative values for the two curves, including the MRE and the standard deviation, are presented in the Table.

Comparison of 10 cm \times 10 cm and 1 cm \times 1 cm dose profiles: MRE and standard deviation

Statistical parameter	$10 \text{ cm} \times 10 \text{ cm}$	1 cm × 1 cm
MRE	5.5 %	50 %
Standard deviation	0.21	0.38

3.2. Analysis of dose profiles using MatriXX Evolution

The MatriXX Evolution detector, with its ionization chamber resolution of 7.62 mm, demonstrated limitations in accurately measuring the dose profiles of the $1 \text{ cm} \times 1 \text{ cm}$ radiation field. The detector's resolution, insufficient to capture the steep dose gradients of such a small field, contributed to significant volume-averaging effects. These effects resulted in a broader profile. Upon analyzing the measurements, it was observed that the actual radiation field size was approximately 14.4 mm instead of the programmed 10 mm (Fig. 7). This discrepancy was confirmed by both Acuros XB calculations and MatriXX Evolution measurements.



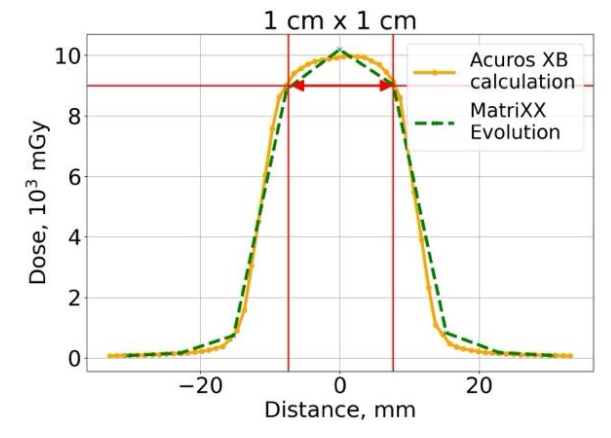


Fig. 7. Comparison of dose profiles: the calculated curve from the TPS and the measured curve from the MatriXX Evolution. As shown by the red arrows on the right plot, the measured field size was 14.4 mm, exceeding the programmed field size of 10 mm. (See color Figure on the journal website.)

The finite size of the radiation source and the mechanical characteristics of the multileaf collimator caused an overlap of penumbrae, which increased the effective field size. From a nuclear physics perspective, this phenomenon arises due to the spatial distribution of photon fluence near the field edges, where secondary scatter contributions and photon attenuation gradients dominate. These effects are particularly pronounced in small fields, where the LCPE is disrupted, further magnifying deviations between the programmed and actual field sizes.

4. Discussion

From a physical perspective, the partial source occlusion changes the spatial distribution of photon fluence within the field. The overlap of penumbrae results in non-uniform beam intensities, which are highly sensitive to the size of the radiation source and the mechanical accuracy of the multileaf collimator. This phenomenon is further influenced by beam hardening effects, where the reduced scatter contributions in smaller fields lead to an increase in the mean photon energy. Consequently, the spectral energy distribution impacts the dose deposition patterns, magnifying the deviations observed in the experimental measurements.

Ref. [1] also highlights the dependence of these effects on the lateral range of charged particles, as the loss of LCPE becomes significant in small fields. The reduced equilibrium amplifies the perturbation effects near the penumbra, further complicating accurate dose measurements. These insights emphasize the need for scrupulous calibration and careful consideration of source occlusion effects when validating dose profiles in small radiation fields.

5. Conclusions

The study evaluated the accuracy of dose profiles for $10 \text{ cm} \times 10 \text{ cm}$ and $1 \text{ cm} \times 1 \text{ cm}$ photon fields

using Gafchromic EBT3 film and MatriXX Evolution detectors. A significant MRE of 49.97 % was observed between the calculated and measured profiles, highlighting the challenges in achieving dosimetric precision in small photon fields. Differences in the penumbra regions, linked to partial source occlusion effects described in [1], further underscored the impact of beam geometry and spectral energy distribution on dose accuracy.

The analysis showed that accurate dose distribution measurements require careful normalization and high-resolution detectors. The Gafchromic EBT3 film's superior spatial resolution enabled a detailed comparison, while the MatriXX Evolution provided reliable data for larger-scale dose verification. However, the MatriXX Evolution's resolution of 7.62 mm, combined with the volume-averaging effect of its ionization chambers, limits its applicability for small field dosimetry. These limitations result in a reduced ability to capture steep dose gradients, making the detector less suitable for fields smaller than the chamber dimensions.

To minimize deviations, it is recommended to incorporate Acuros XB simulations into treatment planning and to select detectors with appropriate resolution and calibration for small photon field dosimetry. Future work should focus on optimizing detector designs and addressing perturbation factors to improve agreement between calculated and measured dose profiles. This study reinforces the importance of following established protocols, such as [1], to enhance the accuracy and reliability of dose measurements in radiotherapy.

The research was partially supported by The National Research Foundation of Ukraine under the project "Improving Quality and Safety in Radiation Therapy for Cancer and Radiological Diagnostics" with registration number 2021.01/0211 (Science for Safety and Sustainable Development of Ukraine).

REFERENCES

- Dosimetry of Small Static Fields Used in External Beam Radiotherapy. Technical Reports Series No. 483 (Vienna, IAEA, 2017) 228 p.
- I.J. Das, G.X. Ding, A. Ahnesjö. Small fields: None-quilibrium radiation dosimetry. Med. Phys. 35 (2008) 206.
- A. Megahed et al. Problems affecting accurate dose measurement in small-field for linear accelerator. Asian Pac. J. Cancer Prev. 24 (2023) 2757.
- G. Neue et al. PantherPix hybrid pixel γ-ray detector for radio-therapeutic applications. J. Instrum. 13 (2018) C02036.
- V. Pugatch et al. Metal micro-detector TimePix imaging synchrotron radiation beams at the ESRF Bio-Medical Beamline ID17. Nucl. Instrum. Methods A 682 (2012) 8.
- B. Henrich et al. PILATUS: A single photon counting pixel detector for X-ray applications. Nucl. Instrum.

- Methods A 607 (2009) 247.
- 7. M.M. Habib et al. Dosimetric investigation of small fields in radiotherapy measurements using Monte Carlo simulations, CC04 ionization chamber, and razor diode. Phys. Eng. Sci. Med. 48 (2025) 813.
- 8. L. Hoffmann et al. Validation of the Acuros XB dose calculation algorithm versus Monte Carlo for clinical treatment plans. Med. Phys. 45 (2018) 3909.
- 9. M. Fuss et al. Dosimetric characterization of GafChromic EBT film and its implication on film dosimetry quality assurance. Phys. Med. Biol. 52 (2007) 4211.
- K.N. Kielar et al. Verification of dosimetric accuracy on the TrueBeam STx: Rounded leaf effect of the high definition MLC. Med. Phys. 39 (2012) 6360.
- M. Yewondwossen, J. Meng. Commissioning brachytherapy TPS using a 2D-array of ion chambers. J. Phys.: Conf. Ser. 250 (2010) 012054.

К. В. Вільчинська^{1,2}, О. А. Безшийко¹, Л. О. Голінка-Безшийко^{1,*}, Р. М. Зелінський³

¹ Київський національний університет імені Тараса Шевченка, Київ, Україна
² Універсальна клініка «Оберіг», Київ, Україна
³ Медичний центр імені академіка Юрія Прокоповича Спіженка, Київ, Україна

*Відповідальний автор: lyalkagb@gmail.com

ПОРІВНЯННЯ ДОЗОВИХ РОЗПОДІЛІВ, ВИМІРЯНИХ РІЗНИМИ ДЕТЕКТОРАМИ У ВЕЛИКИХ ТА МАЛИХ РАДІАЦІЙНИХ ПОЛЯХ

Дослідження порівнює дозові розподіли у великих ($10 \text{ см} \times 10 \text{ см}$) та малих ($1 \text{ см} \times 1 \text{ см}$) радіаційних полях, порівнюючи розрахункові та виміряні дані за допомогою двох різних детекторів. Особлива увага приділяється впливу оклюзії джерела в малих полях та явищу накладення півтіней, як передбачають теоретичні моделі. Малі радіаційні поля, що мають велике значення в клінічній радіаційній терапії, створюють особливі труднощі в дозиметрії через ці ефекти. Результати підкреслюють розбіжності між великими та малими полями, акцентуючи на важливості точних вимірювань та обмеженнях сучасних дозиметричних методик у застосуванні до малих полів.

Ключові слова: променева терапія, контроль якості, детектори, радіохромна плівка, лінійний прискорювач, система планування лікування, розподіл дози.

Надійшла / Received 03.07.2025